

## A failure criterion for RC members under triaxial compression

Hasan Orhun Köksal<sup>†</sup>

*Faculty of Civil Engineering, Yildiz Technical University, 34349 Beşiktaş/Istanbul, Turkey*

*(Received October 4, 2004, Accepted May 13, 2005)*

**Abstract.** The reliable pushover analysis of RC structures requires a realistic prediction of moment-curvature relations, which can be obtained by utilizing proper constitutive models for the stress-strain relationships of laterally confined concrete members. Theoretical approach of Mander is still a single stress-strain model, which employs a multiaxial failure surface for the determination of the ultimate strength of confined concrete. Alternatively, this paper introduces a simple and practical failure criterion for confined concrete with emphasis on introduction of significant modifications into the two-parameter Drucker-Prager model. The new criterion is only applicable to triaxial compression stress state which is exactly the case in the RC columns. Unlike many existing multi-parameter criteria proposed for the concrete fracture, the model needs only the compressive strength of concrete as an independent parameter and also implies for the influence of the Lode angle on the material strength. Adopting Saenz equation for stress-strain plots, satisfactory agreement between the measured and predicted results for the available experimental test data of confined normal and high strength concrete specimens is obtained. Moreover, it is found that further work involving the confinement pressure is still encouraging since the confinement model of Mander overestimates the ultimate strength of some RC columns.

**Keywords:** failure criterion; compressive strength; concrete; column; stress-strain relation.

---

### 1. Introduction

Transverse reinforcement in reinforced concrete members provides lateral confinement to concrete in compression and creates a triaxial compression stress state by increasing the member strength and deformability. The influence of the lateral stress resultants acting in two mutually orthogonal directions to the member axis should be taken into consideration in the modeling of a RC member as a one-dimensional structural frame element. Furthermore the accuracy of a pushover analysis carried out for a RC frame strongly depends on how precisely the ultimate strength and ductility of laterally confined concrete members is determined. Performance based design evidently requires moment-curvature plots obtained from the constitutive relations of confined concrete. This has let researchers and designers use more sophisticated numerical models for the confined concrete (Kent and Park 1971, Skeikh and Uzumeri 1982, Mander *et al.* 1988a, Saatçioğlu and Razvi 1992). However, among these approaches, there exists only a single stress-strain model, which employs a failure criterion for the determination of the confined concrete strength directly. The Mander model

---

<sup>†</sup> Associate Professor, E-mail: [hokksal@yahoo.com](mailto:hokksal@yahoo.com), [koksal@yildiz.edu.tr](mailto:koksal@yildiz.edu.tr)

(1988a) uses the elliptical failure function of William and Warnke (1975) to determine the ultimate strength surface in the Haigh-Westergaard stress space in which the three principal stresses are taken as coordinates. The five-parameter model developed by William-Warnke (1975) needs the knowledge of the concrete strength under uniaxial compression, uniaxial tension, equal biaxial compression and the two high-compressive stress points on the tensile meridian and compressive meridian respectively. It is clear that the only compressive strength among these five material parameters can only be determined experimentally if the emphasis throughout is given on practical aspects of RC design. There are only a limited number of reliable test results (Phillips and Bisheng 1993, Kupfer *et al.* 1969, Richart *et al.* 1928, Balmer 1949) about the determination of the other four parameters and considerable uncertainty exists especially about the last two high-compressive stress points. The experiments of Richart *et al.* (1928) showed that the presence of the uniform lateral pressure resulted an increase in the ratio of confined to unconfined uniaxial strength, equals to approximately 4.1 times the pressure value. Distinctly, Balmer (1949) found the same increment ratio to vary between 4.5 and 7.0 with an average value of approximately 5.6. A more rigid stress-strain behavior is also observed in Balmer's experiments.

In the present paper, a relatively simple and operational failure surface of concrete, applying significant modifications to the two-parameter Drucker-Prager (DP) model (1949), is introduced and illustrated, in order to express both the effect of the confinement pressure on the ultimate strength and the stress-strain relations of confined concrete members under triaxial compression more realistically. Adopting Saenz equation for stress-strain plots, the suggested procedure is compared with the results of the available experimental test data for confined normal and high strength concrete specimens. With reference to this point, when dealing with the different forms of the lateral reinforcement, the effective confinement pressure for a laterally confined RC section is determined using the calculation method recommended by Mander *et al.* (1988a), which is actually an improved form of Skeikh and Uzumeri (1982). Additionally, the full effective lateral pressure assumption is also employed and a detailed comparison between these two approaches is presented.

## 2. Description of failure criterion in principal stress space

The most practical mathematical form of a failure criterion accounting for the effects of both hydrostatic pressure and deviatoric stresses on the ultimate strength is the DP criterion proposed by a simple modification of the von Mises criterion. In the previous studies of the author and his colleagues (Karakoç and Köksal 1997, Köksal *et al.* 2003, 2004, Doran 2004), the DP criterion has been successfully applied to plain concrete specimens, reinforced concrete beams, shear walls, masonry prisms and columns. In order to acquire a better description of the nonlinear volume contradiction behavior of concrete, the simple linear relation of the DP criterion between the hydrostatic pressure and the deviatoric stress component is modified by considering the material parameters  $\alpha$  and  $k$  as functions of the principal stresses as

$$f = \alpha(\sigma_1, \sigma_2, \sigma_3)I_1 + \sqrt{J_2} - k(\sigma_1, \sigma_2, \sigma_3) = 0 \quad (1)$$

where  $\alpha$  represents the plastic dilatation factor. Taking the sign of the compressive stresses as positive throughout the study because of the dominance of the compressive stresses at the case of RC columns, the final form of the proposed failure surface can be expressed in a different way:

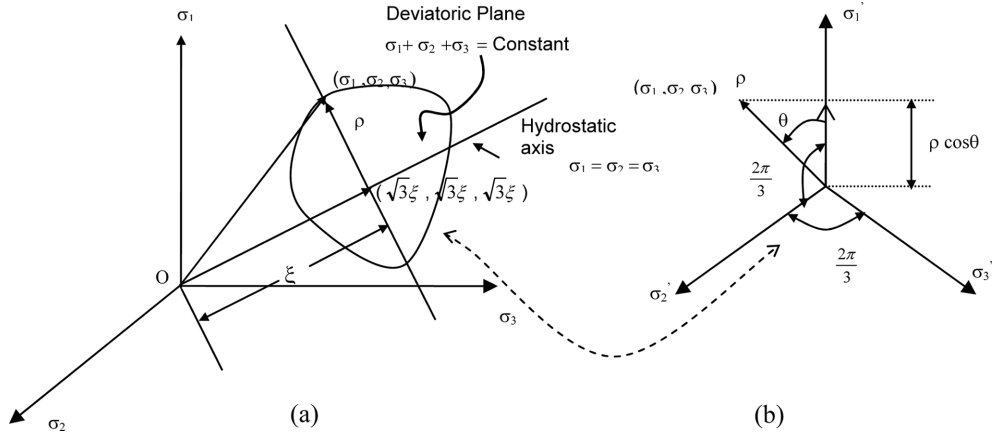


Fig. 1(a) Haigh-Westergaard stress space, (b) Stress state at a point projected on a deviatoric plane (Chen and Han 1988)

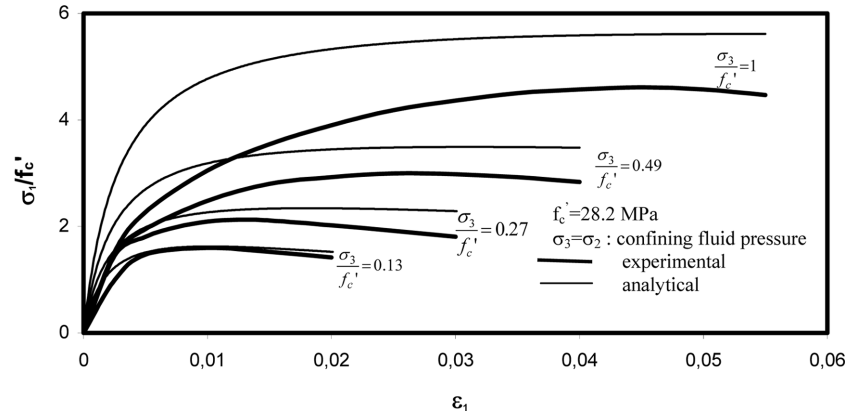


Fig. 2 Plots of the axial stress-strain curves for the triaxial tests of Richart *et al.* (1928)

$$f = \sqrt{6} \alpha(\xi) \xi + \rho - \sqrt{2} k(\sigma_1, \sigma_2, \sigma_3) = 0 \quad (2)$$

where  $\rho(=\sqrt{2J_2})$  and  $\xi(=I_1/\sqrt{3})$  are deviatoric and hydrostatic lengths, respectively, as can be seen in Fig. 1. Initially a constant value is adopted for  $\alpha$  assuming that the coincidence of the surfaces of the Mohr-Coulomb hexagon and the DP cone along the compressive meridian where  $\theta = 60^\circ$

$$\alpha = \frac{2 \sin \phi}{\sqrt{3}(3 - \sin \phi)} \quad (3)$$

and

$$k = \frac{6c \cos \phi}{\sqrt{3}(3 - \sin \phi)} \quad (4)$$

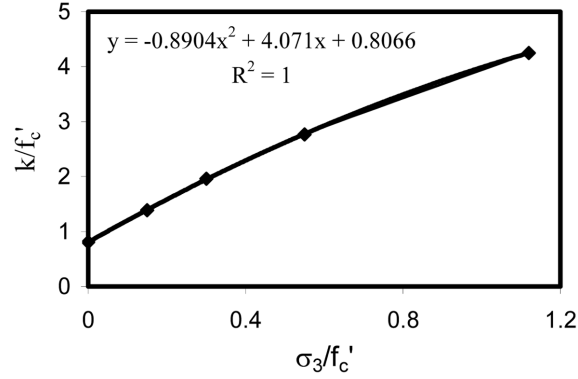


Fig. 3 Fitting of the triaxial compressive strength values for the tests of Richart *et al.* (1928) in Eq. (2)

If an average value of  $30^\circ$  is used for the internal friction angle  $\phi$ , as in the previous studies (Lublimer *et al.* 1989, Karakoç and Köksal 1997),  $\alpha$  can be found as 0.23. After fixing  $\alpha$  at this constant value, a parametric study for the determination of  $k$  has been performed using the test results of Richart *et al.* (1928) illustrated in Fig. 2.  $k$  is considered as a function of the lateral confinement pressure and the cylinder compressive strength of concrete,  $f'_c$  :

$$k = k(\sigma_{lt}, f'_c) \quad (5)$$

where  $\sigma_{lt}$  is the average of the two principal stresses acting in two orthogonal directions to the member axis or the confining fluid pressure in the Richart's tests:

$$\sigma_{lt} = \frac{\sigma_2 + \sigma_3}{2} \quad \text{if } \sigma_1 > \sigma_2 > \sigma_3 \quad (6)$$

Finally, the following expression is obtained by simple curve fitting of the test results as shown in Fig. 3:

$$k = \left( 4.07 \frac{\sigma_{lt}}{f'_c} - 0.89 \left( \frac{\sigma_{lt}}{f'_c} \right)^2 + 0.807 \right) f'_c \quad (7)$$

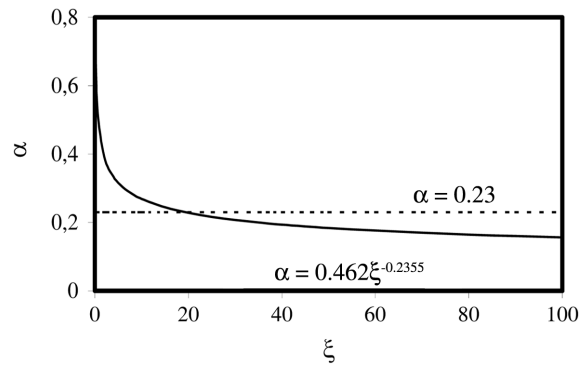


Fig. 4 Variation of  $\alpha$  versus  $\xi$

In order to explain the results of the experimental studies on reinforced concrete columns (Mander *et al.* 1988b, Razvi and Saatçioğlu 1989, Scott *et al.* 1988, Skeikh and Uzumeri 1980) in which the hydrostatic pressure, acting on the core concrete, is in the range of  $0.58 \leq \xi/f'_c \leq 2.00$  for RC column experiments, material parameter  $\alpha$  can be simply expressed in terms of the hydrostatic length:

$$\alpha = \alpha(\xi) = 0.462 \xi^{-0.2355} \quad \text{if } \frac{\xi}{f'_c} \geq 0.58 \quad (8)$$

The ultimate hydrostatic pressure is generally between 20 MPa and 60 MPa during these tests.  $\xi/f'_c \geq 0.58$  draws a reasonable limit for the confined concrete strength under compression implying that the mean compression stress  $\sigma_m = \sqrt{3} \xi = f'_c$ . As can be seen in Fig. 4, a previous constant value assumption for  $\alpha$  as 0.23 seems also reasonable for greater values of hydrostatic pressure than 20 MPa.

The final form of the proposed criterion is obtained by rearranging Eq. (2):

$$f = 1.132 \xi^{0.7645} + \rho - \sqrt{2}k(\sigma_{lr}, f'_c) = 0 \quad (9)$$

The geometrical representation of the proposed criterion is plotted in the principal stress space in Fig. 5. Fig. 6 shows the comparison of the proposed criterion with both the test results of Mills and Zimmerman (1970) and data taken from Ottosen's work (1977) in meridian planes for  $\theta = 0^\circ$  and  $\theta = 60^\circ$  for  $\xi/f'_c \geq 0.58$ . The obtained failure surface is not actually of the DP type anymore. This follows from Fig. 5 and Fig. 6, showing failure surfaces in both the principal stress space and the deviatoric planes depending on the Lode angle, i.e., on the third invariant of the stress state, which is in contrast to the DP criterion. This is clearly an advantage with respect to the DP failure criterion.

In the previous work of the author (Karakoç and Köksal 1997), the cohesion value can be approximated as

$$c = 0.23 \ln(E_0 d_{\max}^2) - 0.60 \quad (10)$$

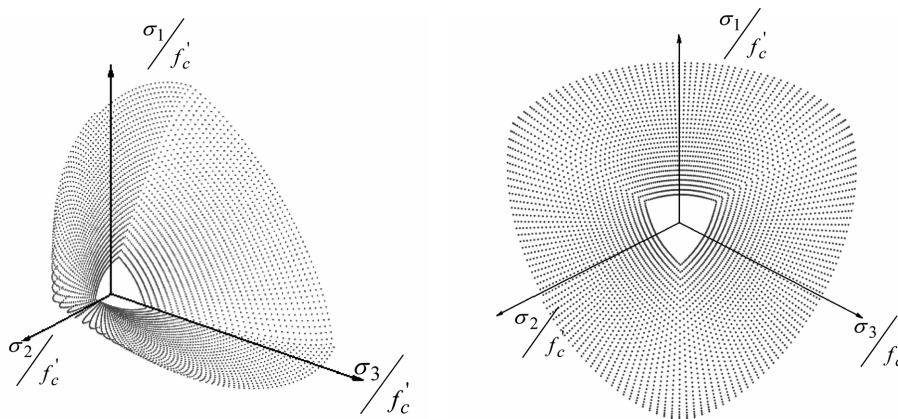


Fig. 5 The geometrical representation of the proposed failure criterion of concrete in the principal stress space

Using Eq. (10) successful applications of the DP criterion to the concrete and reinforced concrete elements are accomplished (Köksal and Karakoç 1997, Doran *et al.* 1998). Considering a normal grade concrete which has a cylindrical compressive strength of 25 MPa, and an initial tangent modulus of 25000 MPa and  $d_{\max} = 20$  mm, one can easily determine  $c$  as 3.05 MPa. If the DP criterion is plotted for these values in Fig. 6, the predictions of the DP criterion are seen much below the measured values for concrete and represent the same straight lines for both tension and compression meridians. The proposed criterion shows the same tendency with the scatter of the experimental data indicating a reasonable end for compression meridian, which has the most governing effect on the ultimate strength of RC elements subjected to tri-axial compression within the specified limits.

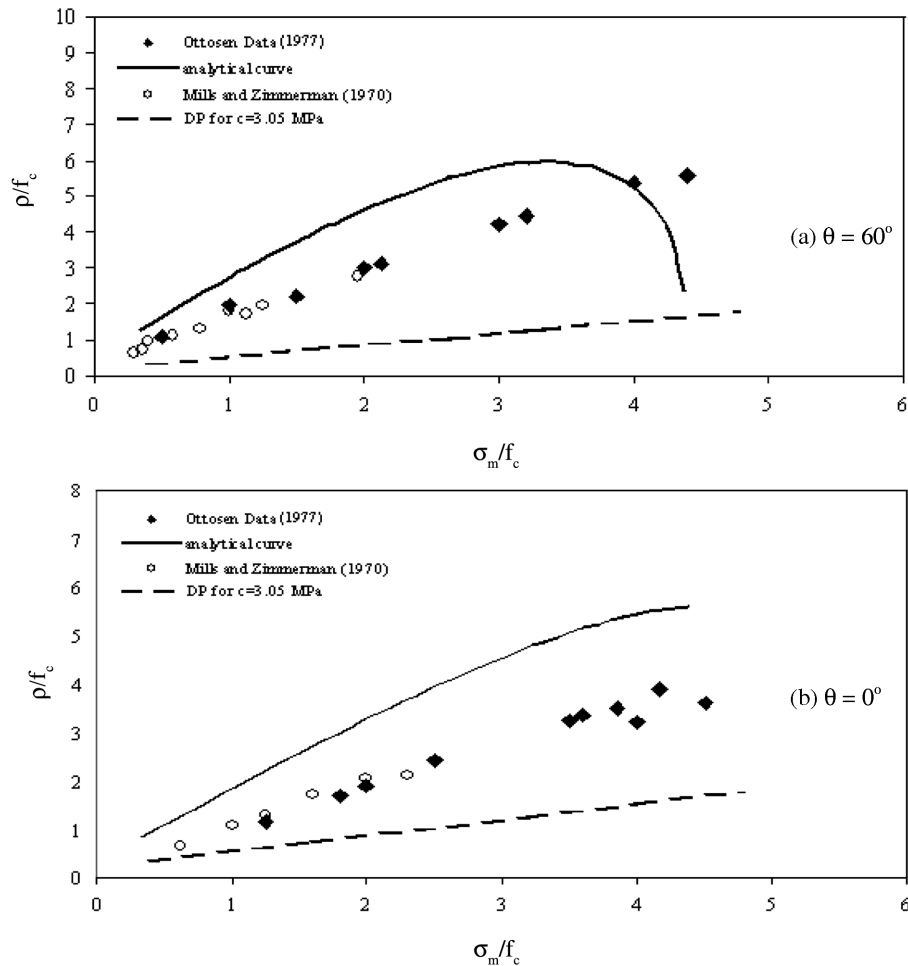


Fig. 6 The geometrical representation of the proposed failure criterion of concrete in the principal stress space for (a)  $\theta = 60^\circ$  and (b)  $\theta = 0^\circ$

### 3. Stress-strain relation of confined concrete

In this study, the Saenz's equation (1964) is adopted for describing the monotonic stress-strain relationship for confined concrete:

$$\sigma_1 = \frac{\varepsilon_1 E_0}{1 + \left(\frac{E_0}{E_s} - 2\right) \frac{\varepsilon_1}{\varepsilon_{cu}} + \left(\frac{\varepsilon_1}{\varepsilon_{cu}}\right)^2} \quad (11)$$

where  $E_0$  is the initial tangent modulus of elasticity in MPa and can be simply taken as  $4750\sqrt{f'_c}$  (Köksal and Arslan 2004),  $E_s$  is the secant modulus at the point of maximum compressive stress  $\sigma_{1u}$  which can be determined using Eqs. (2), (6), (7) and (8).

The strain  $\varepsilon_{cu}$  corresponding to the maximum compressive stress  $\sigma_{1u}$  can be found employing the recommended relations in the pioneering work on the effect of transverse reinforcement on the concrete behavior conducted by Richart *et al.* (1928). Evaluating the test results of 100 mm × 200 mm (4 in. × 8 in.) concrete cylinders subjected to different types of transverse pressure, they concluded that the strength and corresponding strain of concrete were increasingly proportional to the increase in transverse pressure. Based on those early studies, the compression strength of the concrete was expressed as:

$$\sigma_1 = f'_c + k_1 \sigma_3 \quad (12)$$

where  $\sigma_1$  is the compression strength of the concrete with a confining pressure  $\sigma_3$ ;  $f'_c$  is the uniaxial compressive strength; and  $k_1$  is the experimental coefficient, which was proposed as being 4.1 by Richart *et al.* (1928). Balmer (1949) indicates that  $k_1$  is between 4.5 and 7. The peak strain,  $\varepsilon_{cu}$ , corresponding to the compression strength of confined concrete was expressed as:

$$\varepsilon_{cu} = \varepsilon'_c \left(1 + k_2 \frac{\sigma_3}{f'_c}\right) \quad (13)$$

where  $\varepsilon'_c$  is the peak strain at the strength of plain concrete cylinders. Richart *et al.* found  $k_2$  equals to  $5k_1$ . Fig. 2 and Fig. 7 illustrate the fits of triaxial test data obtained by Richardt *et al.* (1928) and

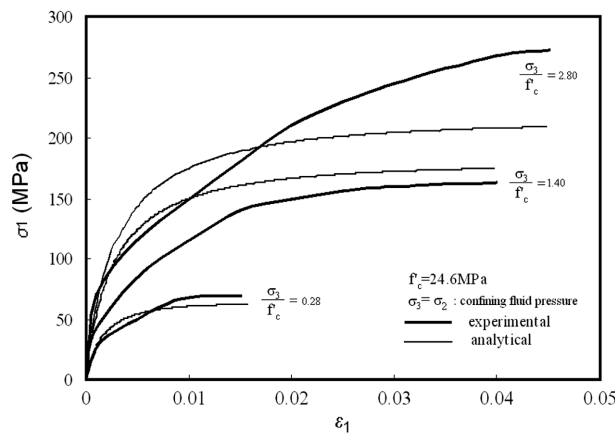


Fig. 7 Fitting of the triaxial tests of Balmer (1949)

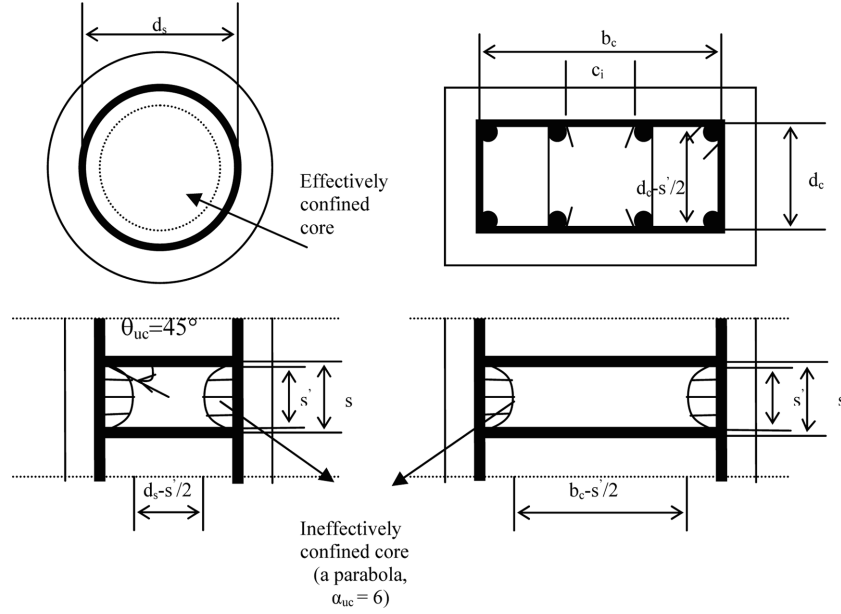


Fig. 8 Effectively confined concrete region in circular, rectangular sections (Mander *et al.* 1988a)

Balmer (1949) respectively. The longitudinal strain is limited to the corresponding experimental maximum value.

#### 4. Application of the model to RC columns

Considerable work has also been done with regard to the behavior of spiral columns and concrete members with circular spirals and rectangular ties. In this study, two approaches are adopted for the determination of the effective lateral confining pressure. The first one is the calculation method recommended in the works of Skeikh and Üzümeri (1982) for effectively confined area and Mander *et al.* (1988a) for the confinement pressure along each side of a column (Fig. 8). Mander *et al.* (1988a) find the effective lateral pressures in two orthogonal directions for rectangular columns as

$$\sigma_{lt,i} = k_e \rho_i f_{yh} \quad i = x, y \quad (14)$$

where  $f_{yh}$  is the yield strength of the transverse reinforcement;  $\sigma_{lt}$  is the lateral confining pressure on concrete; and the effectiveness coefficient  $k_e$ , is given as

$$k_e = \frac{\left( 1 - \frac{\sum_{i=1}^n c_i^2}{\alpha_{uc} b_c d_c} \right) \left( 1 - \frac{s'}{2b_c} \right) \left( 1 - \frac{s'}{2d_c} \right)}{(1 - \rho_{cc})} \quad (15)$$

where  $s'$  is clear vertical spacing between spiral or ties,  $\rho_{cc}$  is ratio of area of longitudinal reinforcement to area of core of section,  $c_i$  is the  $i$ th clear distance between adjacent longitudinal bars,  $b_c$  and  $d_c$  are core dimensions to centerlines of perimeter hoop in  $x$  and  $y$  directions, respectively, where  $b_c \geq d_c$ . In Eq. (15),  $\alpha_{uc}$  is equal to 6 for a parabolic boundary of the ineffective concrete region. For circular spirals, the lateral confinement pressure is also defined by Mander *et al.* (1988a) as:

$$\sigma_{lt} = \frac{1}{2}k_e\rho_s f_{yh} = \frac{1}{2}\left(\frac{1 - \frac{s'}{2d_s}}{(1 - \rho_{cc})}\right)\rho_s f_{yh} \quad (16)$$

The lateral pressure provided by closely spaced circular spirals can be considered to be uniform around the concrete. Therefore, as a second approach for the determination of the confining pressure,  $k_e = 1$  can be adopted for RC columns by assuming all the lateral reinforcement at yield and taking the pressure as uniform around the perimeter of the core. This approach has been also implemented in the confinement model of Saatçioğlu and Razvi (1992) for only circular sections. Actually, there is an uncertainty about the description of lateral pressure exerted by a square and rectangular hoops. Available models are simply based on the calculation of an average value employing some stress distribution patterns (Mander *et al.* 1988a, Saatçioğlu and Razvi 1992) in

Table 1 Strength enhancement in circular columns

No.	Column Label <sup>1</sup>	$\sigma_3$ (MPa) Eq. (16)	$\sigma_3$ (MPa) $k_e = 1$	$f_c^{r1}$ (MPa)	$\sigma_{1,exp}^1$ (MPa)	$\sigma_1^2$ (MPa)	$\sigma_1^3$ (MPa)	$\sigma_1^4$ (MPa)	$\sigma_1^5$ (MPa)	$\frac{\sigma_1^4}{\sigma_{1,exp}}$	$\frac{\sigma_1^5}{\sigma_{1,exp}}$	
1	A	3.01	3.10	30	38	47.75	47.14	46.78	47.31	1.23	1.25	
2	B	3.30	3.40	31	48	50.33	49.50	49.53	50.11	1.03	1.04	
3	C	3.30	3.40	33	47	52.47	51.50	51.76	52.35	1.10	1.11	
4	1	4.18	4.25	28	51	51.40	50.27	51.10	51.51	1.00	1.01	
5	2	2.42	2.55	28	46	42.54	42.57	41.28	41.99	0.90	0.91	
6	3	1.55	1.70	28	40	37.68	38.41	36.35	37.20	0.91	0.93	
7	4	0.86	0.96	28	36	33.55	34.48	32.45	33.03	0.90	0.92	
8	5	3.16	3.20	28	47	46.40	45.59	45.44	45.64	0.97	0.97	
9	6	2.83	3.07	28	46	44.70	45.00	43.58	44.91	0.95	0.98	
10	7	3.35	3.40	31	52	50.62	49.50	49.86	50.11	0.96	0.96	
11	8	3.36	3.40	27	49	46.29	45.50	45.40	45.65	0.93	0.93	
12	9	3.36	3.40	31	52	50.63	49.50	49.87	50.11	0.96	0.96	
13	10	3.35	3.40	27	50	46.27	45.50	45.38	45.65	0.91	0.91	
14	11	3.41	3.40	27	54	46.55	45.50	45.70	45.65	0.85	0.85	
15	12	3.35	3.40	31	52	50.61	49.50	49.84	50.11	0.96	0.96	
										Mean	0.97	0.98
										Std.Dev.	0.09	0.09

<sup>1</sup>Tested by Mander *et al.* (1988b); <sup>2</sup>Mander *et al.* model (1988a), <sup>3</sup>Saatçioğlu and Razvi model (1992); <sup>4</sup>proposed model and Eq. (16), <sup>5</sup>proposed model with  $k_e = 1$

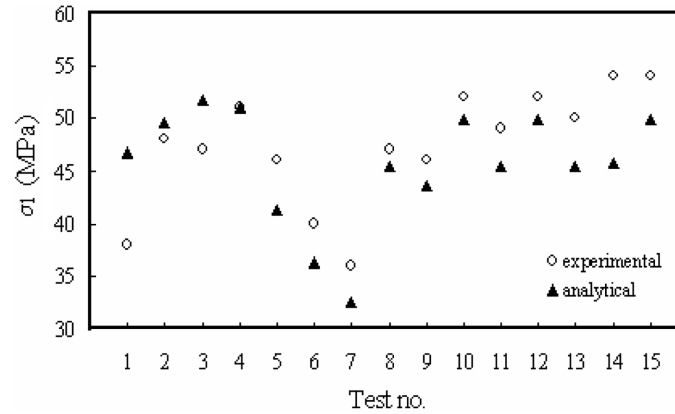


Fig. 9 Strength enhancement in circular columns tested by Mander *et al.* (1988b)

order to deal with this uncertainty. Employing Eqs. (2), (6), (7) and (8) to predict the confined concrete strength, the proposed model is verified by comparing previously recommended relationships with those obtained from 15 circular columns reinforced with spiral and longitudinal reinforcements, which were tested by Mander *et al.* (1988b). Table 1 shows the comparison between the test results and the predictions of the analytical models of Mander *et al.* (1988a), Saatçioğlu and Razvi (1992), and two approaches proposed in this study. Mander *et al.* (1988a) and Saatçioğlu and Razvi (1992) used the experimental values of the compressive strength of unreinforced columns in their analyses. These values are slightly different from the cylindrical compressive strength and actually there is very difficult to test a column instead of a cylinder specimen. Therefore, the cylindrical compressive strength of concrete has been employed throughout this study. As shown in Fig. 9 and Table 1, the predicted to experimental results ratio adopting Eq. (16) is between 0.85 and 1.23, with an average of 0.97 and a standard deviation of 0.09. The ratio is between 0.85 and 1.25, with an average of 0.98 and a standard deviation of 0.09 for the use of the full effective pressure assumption ( $k_e = 1$ ). It appears that adopting the full effective pressure assumption exerted by the circular spirals gives accurate results for the ultimate strength of circular columns.

## 5. Simulation of the compressive behavior of normal and high strength concrete specimens and columns laterally confined with ties under concentric loads

The proposed failure criterion is also verified against the test data of square and rectangular columns, which may have different confinement reinforcement in two orthogonal directions as shown in Tables 2-3. Since the geometry of the square and rectangular columns does not allow a uniform distribution of lateral pressure,  $k$  in Eq. (7) is simply reduced multiplying by 0.85 in order to reflect this geometrical effect just as the same way in the RC design. Alternatively, the full effective lateral pressure ( $k_e = 1$ ) is again employed. Figs. 10-11 illustrate a comparison between the predictions of the proposed model and the experimental results of square (Skeikh and Uzumeri 1980, Scott *et al.* 1982, Razvi and Saatciglu 1989) and rectangular (Mander *et al.* 1988b) columns respectively. For square columns, the predicted to experimental results ratio adopting Eq. (15) is between 0.78 and 1.12, with an average of 0.92 and a standard deviation of 0.09. The same ratio is

Table 2 Strength enhancement in square columns

No.	Column Label <sup>1</sup>	$\sigma_2 = \sigma_3$ (MPa) Eq. (15)	$\sigma_2 = \sigma_3$ (MPa) $k_e = 1$	$f'_c$ (MPa)	$\sigma_{1, \text{exp}}$ (MPa)	$\sigma_1^2$ (MPa)	$\sigma_1^3$ (MPa)	$\frac{\sigma_1^2}{\sigma_{1, \text{exp}}}$	$\frac{\sigma_1^3}{\sigma_{1, \text{exp}}}$
1	2A1-1	0.96	1.82	37.48	37.59	36.44	40.63	0.97	1.08
2	2A1H-2	0.54	1.02	37.00	39.63	33.94	36.27	0.86	0.92
3	4C1-3	1.26	1.86	36.38	37.42	36.85	39.80	0.98	1.06
4	4C1H-4	0.72	1.07	36.65	37.39	34.51	36.20	0.92	0.97
5	4C6-5	4.07	5.67	34.93	48.70	49.24	56.94	1.01	1.17
6	4C6H-6	2.08	2.89	34.31	44.62	38.96	42.90	0.87	0.96
7	4A3-7	2.06	3.95	40.86	44.45	44.96	54.26	1.01	1.22
8	4A4-8	2.12	3.34	40.79	47.15	45.2	51.19	0.96	1.09
9	4A5-9	2.17	4.12	40.51	42.36	45.15	54.76	1.07	1.29
10	4A6-10	3.29	5.27	40.65	45.26	50.8	60.53	1.12	1.34
11	4C3-11	1.62	2.90	40.65	43.88	42.6	48.90	0.97	1.11
12	4C4-12	2.68	3.56	40.79	50.62	47.95	52.27	0.95	1.03
13	4A1-13	1.07	1.90	31.28	34.57	31.27	35.29	0.90	1.02
14	2A5-14	2.54	5.10	31.49	36.93	38.5	50.87	1.04	1.38
15	2A6-15	2.82	4.80	31.69	39.60	40.1	49.64	1.01	1.25
16	4C1-16	1.47	2.24	32.52	37.59	34.32	38.08	0.91	1.01
17	2C5-17	2.18	4.12	32.87	37.99	38.1	47.49	1.00	1.25
18	2C6-18	4.36	6.26	33.07	47.79	48.84	57.95	1.02	1.21
19	4B3-19	1.88	3.60	33.42	40.62	37.15	45.50	0.91	1.12
20	4B4-20	3.19	4.63	34.66	44.78	44.67	51.66	1.00	1.15
21	4B6-21	3.91	5.87	35.48	46.45	48.95	58.44	1.05	1.26
22	4D3-22	1.77	3.09	35.48	43.43	38.51	44.97	0.89	1.04
23	4D4-23	3.23	4.51	35.83	46.90	46.00	52.20	0.98	1.11
24	4D6-24	3.79	5.47	35.83	49.64	48.72	56.85	0.98	1.15
25	2	2.05	2.81	25.30	33.00	30.49	34.10	0.92	1.03
26	6	1.70	2.69	25.30	32.40	28.85	33.52	0.89	1.03
27	12	1.46	2.16	30.30	40.40	32.25	35.65	0.80	0.88
28	13	2.05	2.81	30.30	43.00	35.10	38.77	0.82	0.90
29	14	2.42	3.46	30.30	43.50	36.87	41.89	0.85	0.96
30	15	3.58	4.77	30.30	48.50	42.47	48.17	0.88	0.99
31	17	1.21	2.07	30.30	38.50	31.06	35.20	0.81	0.91
32	18	1.70	2.69	30.30	41.70	33.42	38.18	0.80	0.92
33	19	1.91	3.15	30.30	42.20	34.44	40.41	0.82	0.96
34	20	2.83	4.34	30.30	45.60	38.85	46.08	0.85	1.01
35	22	1.46	2.16	29.50	35.80	31.52	34.91	0.88	0.98
36	23	2.05	2.81	29.50	37.90	34.36	38.02	0.91	1.00
37	24	2.42	3.46	29.50	39.90	36.13	41.13	0.91	1.03
38	25	3.58	4.77	29.50	45.50	41.70	47.40	0.92	1.04

Table 2 Continued

No.	Column Label <sup>1</sup>	$\sigma_2 = \sigma_3$ (MPa) Eq. (15)	$\sigma_2 = \sigma_3$ (MPa) $k_e = 1$	$f'_c$ (MPa)	$\sigma_{1, \text{exp}}$ (MPa)	$\sigma_1^2$ (MPa)	$\sigma_1^3$ (MPa)	$\frac{\sigma_1}{\sigma_{1, \text{exp}}}$ <sup>2</sup>	$\frac{\sigma_1}{\sigma_{1, \text{exp}}}$ <sup>3</sup>
39	3(a)	2.05	5.00	32.00	40.00	36.70	50.88	0.92	1.27
40	3(b)	2.05	5.00	32.00	38.40	36.70	50.88	0.96	1.33
41	4(a)	0.71	2.50	32.00	33.30	30.22	38.85	0.91	1.17
42	6(a)	1.88	5.18	39.00	51.90	42.32	58.53	0.82	1.13
43	6(b)	1.88	5.18	39.00	51.10	42.31	58.53	0.83	1.15
44	7(a)	0.65	2.59	39.00	43.30	36.30	45.83	0.84	1.06
45	7(b)	0.65	2.59	39.00	44.80	36.31	45.83	0.81	1.02
46	15(a)	0.71	2.50	29.00	35.10	27.50	36.06	0.78	1.03
47	15(b)	0.71	2.50	29.00	31.60	27.50	36.06	0.87	1.14
48	16(a)	2.05	5.00	29.00	31.60	33.92	47.97	1.07	1.52
49	16(b)	2.05	5.00	29.00	31.60	33.92	47.98	1.07	1.52
Mean								0.92	1.11
Std.Dev.								0.09	0.15

<sup>1</sup>2A-1-4D-24 tested by Sheikh and Üzümeri (1980). 2-25 (12-25 tested under high strain rate of 0,0167/s) tested by Scott *et al.* (1982). 3(a)-16(b) Razvi and Saatçioğlu (1992); <sup>2</sup>proposed model and Eq. (15); <sup>3</sup>proposed model with  $k_e = 1$

Table 3 Strength enhancement in rectangular columns

No.	Column Label <sup>1</sup>	$\sigma_{it}^1$ (MPa) Eq. (15)	$\sigma_{it}^1$ (MPa) $k_e = 1$	$f'_c$ (MPa)	$\sigma_{1, \text{exp}}^1$ (MPa)	$\sigma_1^2$ (MPa)	$\sigma_1^3$ (MPa)	$\frac{\sigma_1}{\sigma_{1, \text{exp}}}$ <sup>2</sup>	$\frac{\sigma_1}{\sigma_{1, \text{exp}}}$ <sup>3</sup>
1	1.00	4.71	7.25	28.00	46.00	45.65	57.52	0.99	1.25
2	2.00	5.15	7.92	28.00	56.00	47.73	60.64	0.85	1.08
3	3.00	3.58	5.51	28.00	46.00	40.29	49.41	0.88	1.07
4	4.00	4.30	6.62	28.00	51.00	43.71	54.59	0.86	1.07
5	5.00	1.14	1.75	28.00	37.00	28.63	31.57	0.77	0.85
6	6.00	6.86	10.55	28.00	56.00	55.73	72.56	1.00	1.30
7	9.00	5.16	7.94	41.00	72.00	60.33	73.86	0.84	1.03
8	10.00	5.56	8.55	41.00	72.00	62.29	76.83	0.87	1.07
9	11.00	2.32	3.57	41.00	60.00	46.36	52.52	0.77	0.88
10	12.00	8.08	12.43	41.00	78.00	74.55	95.27	0.96	1.22
11	13.00	5.65	8.69	41.00	69.00	62.73	77.50	0.91	1.12
12	14.00	2.08	3.20	41.00	58.00	45.18	50.70	0.78	0.87
Mean								0.87	1.07
Std.Dev.								0.08	0.14

<sup>1</sup>Tested by Mander *et al.* (1988b); <sup>2</sup>proposed model and Eq. (15), <sup>3</sup>proposed model with  $k_e = 1$

between 0.88 and 1.52, with an average of 1.11 and a standard deviation of 0.15 for the use of the full effective pressure assumption ( $k_e = 1$ ). For rectangular columns, the mean values for the

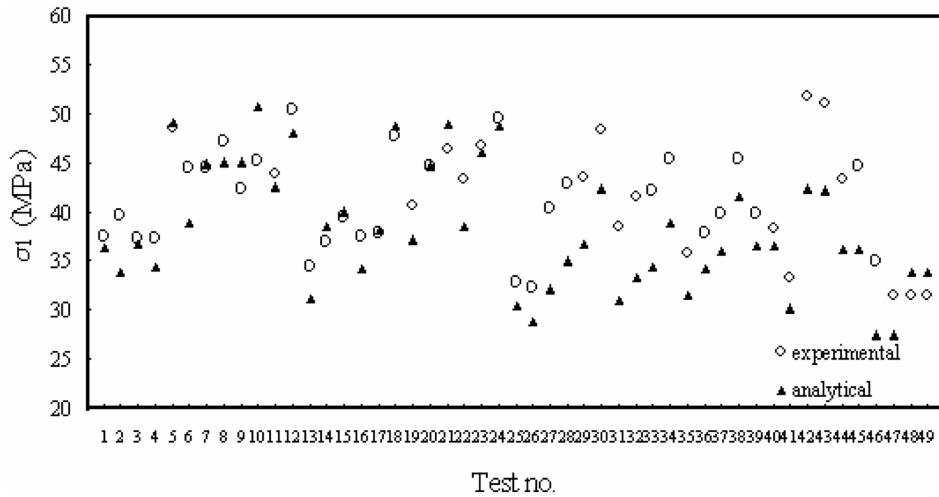


Fig. 10 Strength enhancement in square columns (1-24 tested by Sheikh and Üzümeri (1980); 25-38 tested by Scott *et al.* (1988); 39-49 tested by Razvi and Saatçioğlu (1989))

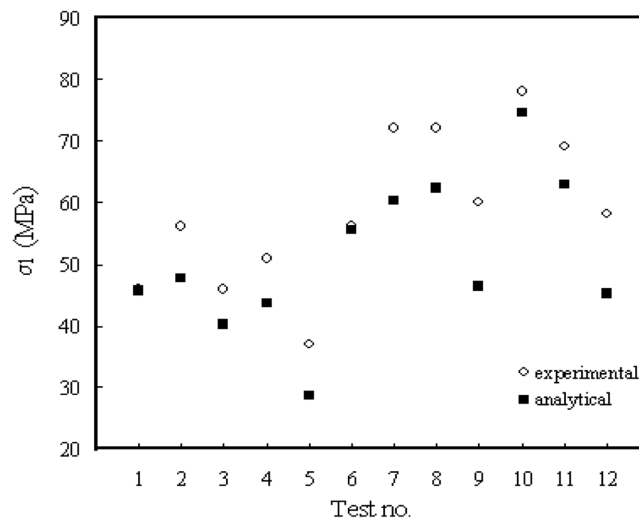


Fig. 11 Strength enhancement in rectangular columns tested by Mander *et al.* (1988b)

predicted to experimental results ratio are finally determined as 0.87 and 1.07 and the standard deviations are 0.08 and 0.14 respectively. The better predictions are obtained for the determination of the ultimate strength of square and rectangular columns utilizing the confinement model recommended by Mander *et al.* (1988a) rather than assuming the full effective pressure. As can be seen from the plots of the axial stress-strain relations of the columns in Figs. 12-14 tested by Mander *et al.* (1988b) by using Eqs. (2), (6), (7) and (8), the predictions of both approaches proposed in this study are well agreement with the experimental results for the square and circular RC columns.

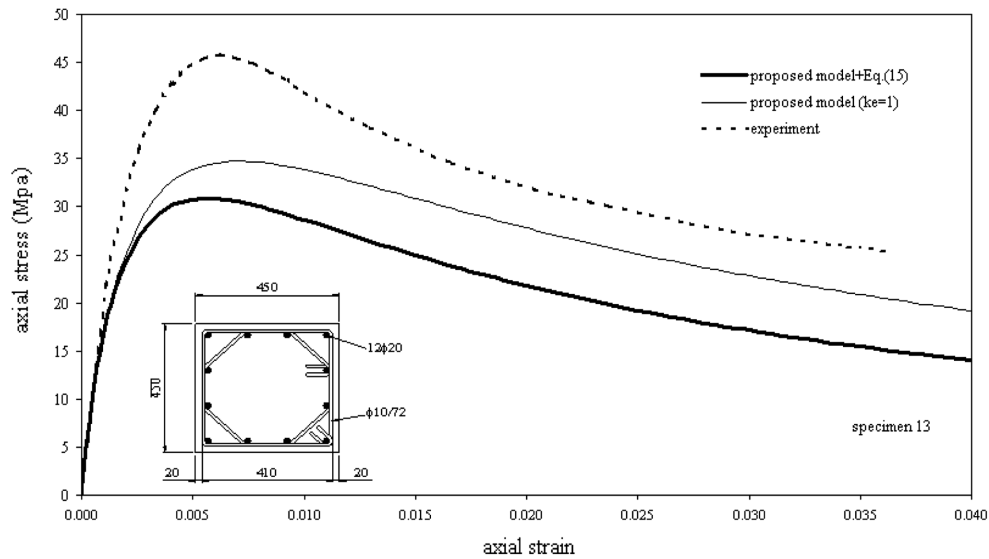
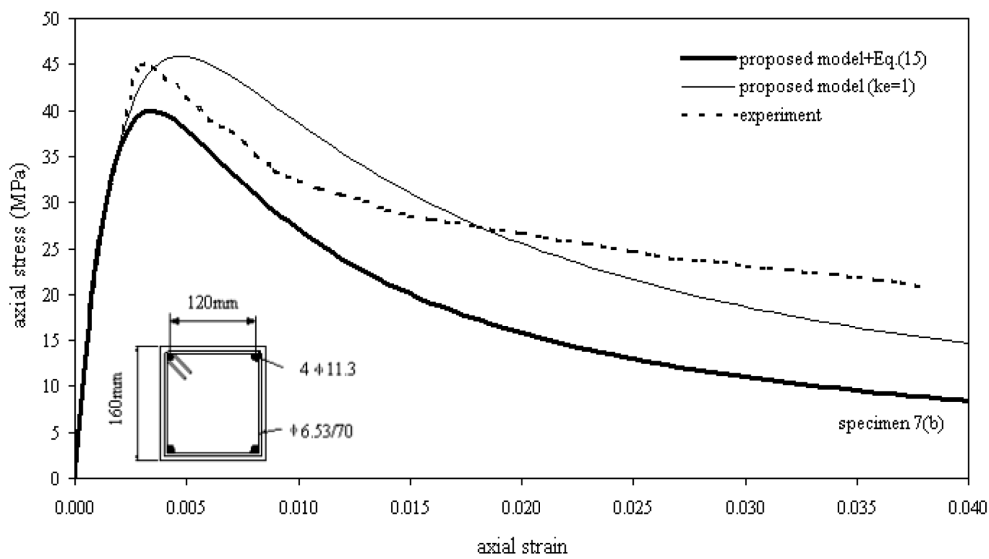
Fig. 12 Fitting of specimen 13 tested by Mander *et al.* (1988b)

Fig. 13 Fitting of specimen 7 tested by Razvi and Saatçioğlu (1988)

Due to the increasing use of high strength concrete (HSC) in structures such as buildings, bridges, and offshore platforms, there is a continuing effort of understanding the behavior of HSC under confined compression. Hsu and Hsu (1994) investigated the complete stress-strain behavior of HSC under compression. HSC specimens having three different tie spacing ( $s = 2.54$  cm, 5.08 cm and 7.62 cm) were tested under uniaxial compression and complete axial stress-strain curves are plotted. The proposed model using Eq. (16) for the effective lateral pressure also leads to reasonable predictions for these three specimens in Fig. 15.

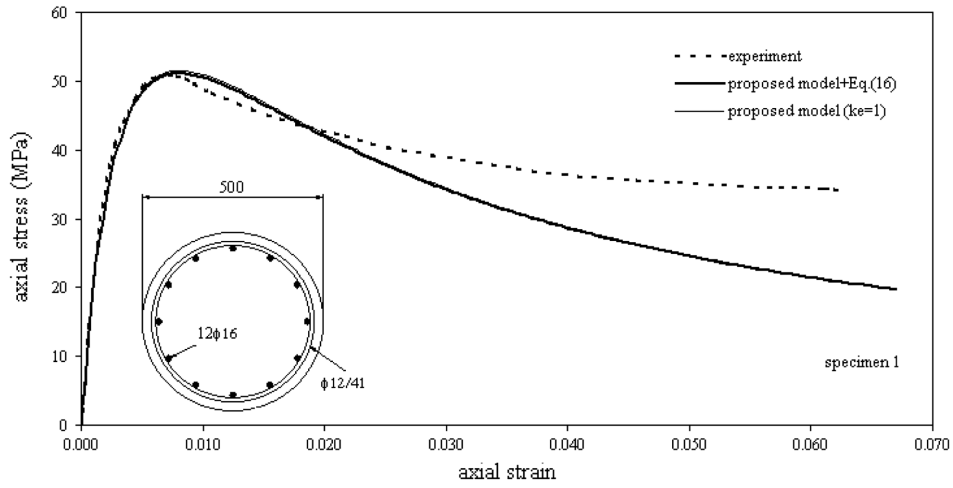


Fig. 14 Fitting of specimen 1 tested by Mander *et al.* (1988b)

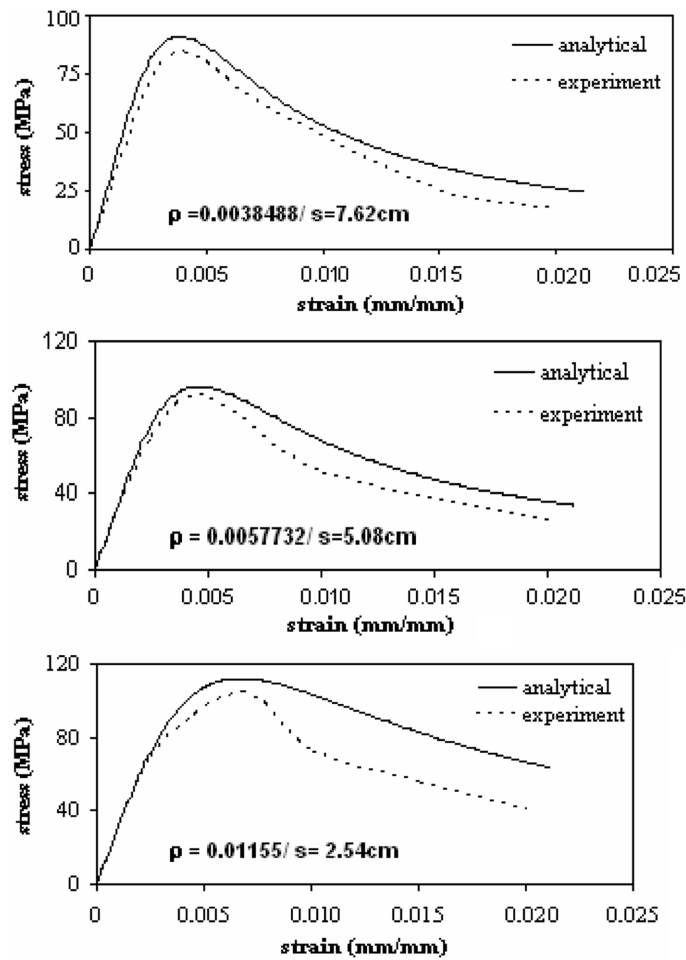


Fig. 15 Fitting of high strength concrete specimens tested by Hsu and Hsu (1994)

Table 4 Comparison of experimental and analytical  $\sigma_1$  values in square columns tested by Chung *et al.* (2002)

Column label	$\sigma_2 = \sigma_3$ (MPa) Eq. (15)	$f'_c$ (MPa)	$\sigma_{1, \text{exp}}$ (MPa)	$\sigma_1^1$ (MPa)	$\sigma_1^2$ (MPa)
L8S5.5S3	4.76	20	29.90	44.74	38.10
L8S5.5S5.5	2.18	20	21.40	32.73	26.24
L8S5.5S10	0.83	20	18.00	25.31	19.97
H8S5.5S3	4.76	54	56.92	82.52	70.84
H8S5.5S5	2.18	54	48.65	67.91	57.86
H8S5.5S10	0.83	54	42.69	59.53	51.07
L8S5.5E3	8.65	20	37.06	59.90	55.25
L8S5.5E5.5	3.87	20	26.86	40.84	34.04
L8S5.5E10	1.53	20	18.70	29.28	23.22
H8S5.5E3	8.65	54	64.72	101.95	90.27
H8S5.5E5	3.87	54	52.33	77.64	54.59
H8S5.5E10	1.53	54	37.18	63.94	66.36
L12S5.5E3	9.28	20	35.70	62.16	57.92
L12S5.5E5.5	4.24	20	24.65	42.47	35.73
L12S5.5E10	1.62	20	17.51	29.76	23.64
H12S5.5E3	9.28	54	64.26	104.91	93.39
H12S5.5E5	4.24	54	55.54	79.68	68.23
H12S5.5E10	1.62	54	48.20	64.49	55.04

<sup>1</sup>Mander *et al.* (1988a)'s model; <sup>2</sup>proposed model and Eq. (15).

Chung *et al.* (2002) tested sixty-five reinforced concrete columns with a 200 mm square cross sections. Table 4 shows the ultimate strength values of eighteen column having simple tie configurations among the test specimens and the predictions of both the proposed criterion and Mander model. L and H series have the compressive strength of 20 and 54 MPa. The numbers 8 and 12 that follow L and H denote 8-No. 4 and 12-No. 3 longitudinal reinforcement. The letter S after the numbers denotes the simple type of confinement tie. The number 5.5 indicates the yield strength of ties of 550 MPa. The letters S and E represent the diameters of 6 and 8 mm, respectively, and the last numbers 3, 5.5, and 10 represent the tie spacing in centimeters. The predictions of the proposed failure criterion and Mander's theoretical model for the ultimate strengths of these eighteen RC columns are respectively 11% to 54% and 22% to 72% higher compared to the test results. If the diameter of lateral ties is increased, the available confining models always yield greater lateral pressures and the increased ultimate load capacity for RC columns in the confinement model of Mander (1988a). The high lateral pressure values obtained using this model can be the main reason for high prediction values. Moreover, Chung *et al.* (2002) presents some contradictory results about the effects of increasing tie diameter. The ultimate strength of H8S5.5E10 is 13% less than the ultimate strength of H8S5.5S10 although the proposed model estimates a 7% increase. The author (Köksal *et al.* 2004) previously carried out three-dimensional nonlinear analyses of the grouted masonry columns and made a notification about the fact that the effect of the lateral tie diameter on the ultimate load should be considered together with the diameter of the vertical reinforcement bars. Therefore, the confinement models should take into account the effect of tie diameter in detail instead of employing simplified stress distribution patterns for the lateral pressure.

## 6. Conclusions

In this study, introducing significant modifications into the Drucker-Prager model, a new failure criterion, accounts for the influence of the confinement on the ultimate strength, is proposed for the triaxial compressive stress state, which is exactly the case in the RC columns. Unlike many existing multi-parameter models for representing concrete fracture, the new model needs only the cylinder compressive strength of concrete as an independent parameter. The crucial point for the stress-strain models for the confined concrete is the determination of the confinement pressure exerted by the different forms of the lateral reinforcement. In this study, the calculation method recommend by Mander *et al.* (1988a) is adopted for the determination of the effective confinement pressure. Besides, the full effective lateral pressure assumption is also employed as an alternative approach. A detailed comparison between these two approaches shows a slight difference, and good agreements are obtained for the experimental results of circular column sections. For square and rectangular sections, it is found that there is a slight advantage of the Mander confinement model over the assumption of the full effective pressure. The proposed model also leads to reasonable predictions for three high strength concrete specimens under axial pressure tested by Hsu and Hsu (1994). However, the ultimate strengths of the RC columns tested by Chung *et al.* (2002), are overestimated by both the proposed model and Mander's theoretical model. The reason for that are the high lateral confinement pressure values obtained from the calculations of the confinement model. Further work involving the realistic distribution patterns of confinement pressure arising from the different type of lateral reinforcement is still encouraging. Finally, adopting Saenz equation for the stress-strain plots, the validity of the proposed model has been shown by comparisons with the test data of plain concrete and reinforced concrete specimens.

## References

- Balmer, G.G. (1949), *Shearing Strength of Concrete under High Triaxial Stress-Computations of Mohr's Envelope as a Curve*, Structural Research Laboratory Report SP:23, US Bureau of Reclamation, Denver.
- Chen, W.F. and Han, D.J. (1988), *Plasticity for Structural Engineers*, Springer-Verlag, New York.
- Chung, H.S., Yang, K.H., Lee, Y.H. and Eun, H.C. (2002), "Strength and ductility of laterally confined concrete columns", *Can. J. Civ. Eng.*, **29**(6), 820-830.
- Doran, B., Köksal, H.O., Polat, Z. and Karakoç, C. (1998), "Betonarme Elemanlarda Sonlu Eleman Uygulamalarında Drucker-Prager Akma Kriterlerinin Kullanılması", *IMO Teknik Dergi*, **9**(2), 1617-1625.
- Doran, B. (2004), "Elastic-plastic analysis of R/C coupled shear walls: The equivalent stiffness ratio of the tie elements", *J. Indian Inst. of Sci.*, **83**(3-4), 87-94.
- Drucker, D.C. (1949), "Relation of experiments to mathematical theories of plasticity", *J. Appl. Mech.*, ASME, **16**, 349-357.
- Hsu, L.S. and Hsu, C.T.T. (1994), "Complete stress-strain behaviour of high strength concrete under compression", *Mag. Concr. Res.*, **46**(169), 301-312.
- Kent, D.C. and Park, R. (1971), "Flexural members with confined concrete", *J. Struct. Eng.*, ASCE, **97**(7), 1969-1990.
- Karakoç, C. and Köksal, H.O. (1997), "The modeling of concrete fracture", *Studi e Ricerche, Politecnico di Milano*, **18**, 271-283.
- Köksal, H.O., Karakoç, C. and Yıldırım, H. (2003), "Compressive strength of concrete hollow-block masonry", *Studi e Ricerche, Politecnico di Milano*, **24**, 189-206.
- Köksal, H.O., Doran, B., Özsoy, E. and Alacalı, S.N. (2004), "Nonlinear modeling of concentrically loaded reinforced blockwork masonry columns", *Canadian J. Civil Eng.*, **31**(6), 1012-1023.

- Köksal, H.O. and Arslan, G. (2004), "Damage analysis of RC beams without web reinforcement", *Mag. Concr. Res.*, **56**(4), 231-242.
- Lubliner, J., Oliver, J., Oller, S. and Onate, E. (1989), "A plastic damage model for concrete", *Int. J. Solids Struct.*, **25**(3), 299-326.
- Mander, J.B., Priestley, M.J.N. and Park, R. (1988a), "Theoretical stress-strain model for confined concrete", *J. Struct. Eng.*, ASCE, **114**(8), 1804-1826.
- Mander, J.B., Priestley, M.J.N. and Park, R. (1988b), "Observed stress-strain behavior of confined concrete", *J. Struct. Eng.*, ASCE, **114**(8), 1827-1849.
- Mills, L.L. and Zimmerman, R.M. (1970), "Compressive strength of plain concrete under multi-axial loading conditions", *ACI J.*, **67**(10), 802-807.
- Ottosen, N.S. (1977), "A failure criterion for concrete", *J. Eng. Mech. Div.*, ASCE, **103**(4), 527-535.
- Phillips, D.V. and Bisheng, Z. (1993), "Direct tension tests on notched and unnotched plain concrete specimens", *Mag. Concr. Res.*, **45**(162), 25-35.
- Razvi, S.R. and Saatçioğlu, M. (1989), "Confinement of reinforced concrete columns with welded wire fabric", *ACI Struct. J.*, **86**(5), 615-623.
- Richart, F.E., Brandtzaeg, A. and Brown, R.L. (1928), "A study of the failure of concrete under combined compressive stresses", Bul 185, Univ. Illinois, Eng. Experimental Station, Champaign, III.
- Saatçioğlu, M. and Razvi, S.R. (1992), "Strength and ductility of confined concrete", *J. Struct. Eng.*, ASCE, **118**(6), 1590-1607.
- Saenz, L.P. (1964), "Discussion of "Equation for the stress-strain curve of concrete" by Desayi and Krishnan", *ACI J.*, **61**(9), 1229-1235.
- Scott, B.D., Park, R. and Priestly, M.J.N. (1982), "Stress-strain behavior of concrete confined by overlapping hoops at low and high strain rates", *ACI J.*, **79**(1), 13-27.
- Skeikh, S.A. and Uzumeri, S.M. (1980), "Strength and ductility of tied concrete columns", *J. Struct. Eng.*, ASCE, **106**(5), 1079-1102.
- Skeikh, S.A. and Uzumeri, S.M. (1982), "Analytical model for concrete confinement in tied columns", *J. Struct. Eng.*, ASCE, **108**(12), 2703-2722.
- William, K.J. and Warnke, E.P. (1975), "Constitutive model for the triaxial behavior of concrete", *Proc. Int. As. for Bridge and Struct. Eng.*, **19**, 1-30.

## Notation

$\alpha$	: plastic dilatation factor
$\sigma_1, \sigma_2, \sigma_3$	: principal stresses
$\sigma_l$	: lateral confining pressure
$\rho$	: deviatoric length
$\xi$	: hydrostatic length
$b_c$	: concrete core dimension to center line of perimeter hoop in x-direction
$d_c$	: concrete core dimension to center line of perimeter hoop in y-direction
$d_s$	: diameter of spiral
$f'_c$	: compressive strength of concrete cylinder
$s'$	: clear vertical spacing between spiral and/or ties
$E_0$	: initial modulus of elasticity
$E_s$	: secant modulus of elasticity
$I_1$	: first invariant of stress tensor
$J_2$	: second invariant of stress deviator tensor